DOI: 10.1002/ejic.200700935

Synthesis and Structural Characterisation of *cis*- and *trans*-$[(hppH)_2PtCl_2]$, $[(hppH)_3PtCl]^+Cl^-$ and Some New Salts of the $[hppH_2]^+$ Cation (hppH = 1,3,4,6,7,8-Hexahydro-2*H*-pyrimido[1,2-*a*]pyrimidine): The Importance of Hydrogen Bonding

Ute Wild,[a] Pascal Roquette,[a] Elisabeth Kaifer,[a] Jürgen Mautz,[a] Olaf Hübner,[a] Hubert Wadepohl,[a] and Hans-Jörg Himmel*[a]

Keywords: Platinum / Hydrogen bonding / Quantum chemical calculations / N ligands

The reaction between the guanidine derivative hppH (hppH = 1,3,4,6,7,8-hexahydro-2*H*-pyrimido[1,2-*a*]pyrimidine) and K_2PtCl_4 in H_2O affords the salt $[hppH_2]_2[PtCl_4]$, which reacts further with Li(hpp) in thf to give *cis*-$[(hppH)_2PtCl_2]$. The corresponding *trans* isomer is obtained from the reaction between $[(dmso)_2PtCl_2]$ and hppH. hppH easily replaces another chlorido ligand to give $[(hppH)_3PtCl]^+Cl^-$. $[hppH_2]Cl$ is formed as a hygroscopic side-product in the synthesis of $[(hppH)_2PtCl_2]$ and takes up 1 equiv. of H_2O to give $[hppH_2]Cl{\cdot}H_2O$. We report the crystal structures of *cis*- and *trans*-$[(hppH)_2PtCl_2]$, $[(hppH)_3PtCl]^+Cl^-$ and some salts of the $[hppH_2]^+$ cation, namely $[hppH_2]_2[PtCl_4]$ and the Pt-free salts $[hppH_2][BPh_4]$, $[hppH_2]Cl$ and $[hppH_2]Cl{\cdot}H_2O$, which have an increasing degree of directed intermolecular hydrogen contacts. The crystal structure of $[hppH_2]Cl{\cdot}H_2O$ features helical chains of $Cl^-{\cdot}H_2O$ connected via $[hppH_2]^+$ cations. The effects of hydrogen bonding on the structures of these compounds in the solid state are discussed. Finally, quantum chemical calculations provide further insight into the structures and properties of some of these compounds.

Introduction

cis-$[(NH_3)_2PtCl_2]$ (cisplatin, **1**) is a well-known, 16-valence-electron complex which has attracted considerable attention due to its cytostatic properties. Intermolecular interactions, including H···Cl and Pt···Pt contacts (distances of 337.2/340.9 pm), are important in this complex in the crystalline phase.[1] According to quantum chemical calculations (B3LYP/6-31G**) and using a model consisting of four molecules, the intermolecular interactions in *cis*-$[Pt(NH_3)_2Cl_2]$ were estimated to be of the order of 360 kJ mol^{-1}.[2] The *trans* form of the molecule is more stable than the *cis* form, and the *trans*–*cis* energy difference has been calculated to be –55, –76, –55 and –57 kJ mol^{-1} by B3LYP,[2] HF,[3] MP2[4] and G3 methods, respectively. Intermolecular H···Cl interactions are also present in the *trans* form, although there are no Pt···Pt interactions.[1]

According to recent quantum chemical calculations, the Pt–NH_3 bond in cisplatin is around 50 kJ mol^{-1} stronger than the Pt–Cl bond.[5] Nevertheless, it has been shown that the Pt^{II} complex $[Pt(NH_3)_3Cl]Cl$ cannot easily be obtained in high yield as the direct reaction between *cis*- or *trans*-$[Pt(NH_3)_2Cl_2]$ and 1 mol-equiv. of NH_3 or, under forcing conditions, of $[Pt(NH_3)_4]^{2+}$ with 1 mol-equiv. of Cl^-, always results in mixtures of $[Pt(NH_3)_2Cl_2]$, $[Pt(NH_3)_3Cl]Cl$ and $[Pt(NH_3)_4]Cl_2$.[6] The best method for synthesising $[Pt(NH_3)_3Cl]Cl$ is probably that reported in 1948,[7] where *cis*-$[Pt(NH_3)_2Cl_2]$ is first treated with K_2PtCl_4 to obtain a mixture of Cleve's pink salt $[Pt(NH_3)_3Cl]_2[PtCl_4]$ and Magnus' green salt $[Pt(NH_3)_4][PtCl_4]$. The higher solubility of Cleve's salt in hot water can be used to separate these two compounds. Subsequent treatment of Cleve's salt with $[Pt(NH_3)_4]Cl_2$ finally yields the desired $[Pt(NH_3)_3Cl]Cl$ together with $[Pt(NH_3)_2][PtCl_4]$, which precipitates from the reaction mixture.

Exchange of the ammonia ligands in $[(NH_3)_2PtCl_2]$ with other nitrogen bases has led to several interesting complexes. For example, the compound $[\eta^2$-(2,2′-bipyrimidyl)]-dichloridoplatinum(II) $[(bpym)PtCl_2]$ (**2**; Scheme 1) has been used to oxidise methane to a methanol derivative in a one-pass yield of 70%.[8] However, since the reaction proceeds in concentrated, hot H_2SO_4, the lifetime of the Pt catalyst is limited to about 15 min, and precipitation of insoluble $PtCl_2$ is observed. Molecules of this complex have been shown to be linked through Pt···Pt contacts [337.1(1)/341.1(1) pm] in the solid state,[9] with a Pt···Pt···Pt angle of 162.55(2)°. More recently, $[(N\text{-}N)Pt(CH_3)(OH_2)]^+[BF_4]^-$ (**3**), where N-N is a 3,5-bis(trifluoromethyl)phenyl-substituted diimine, has been synthesised and been shown to activate hydrocarbons (e.g. benzene or methane) under mild condi-

[a] Anorganisch-Chemisches Institut, Ruprecht-Karls-Universität Heidelberg
Im Neuenheimer Feld 270, 69120 Heidelberg, Germany
E-mail: hans-jorg.himmel@aci.uni-heidelberg.de

tions in 2,2,2-trifluoroethanol.[10] The mechanism for this reaction was studied using the model systems cis- and transplatin and with the aid of quantum chemical calculations.[11]

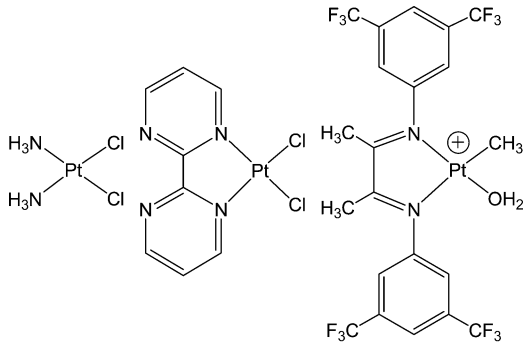

1 **2** **3**

Scheme 1.

The nitrogen base 1,3,4,6,7,8-hexahydro-2*H*-pyrimido[1,2-*a*]pyrimidine (hppH, **4**) is a much stronger base than NH_3[12] and should also form stable complexes with Ni, Pd and Pt (M) of the formula [(hppH)$_2$MCl$_2$]. Interestingly, although not unprecedented for guanidines or amidines,[13] the crystal structure of uncoordinated hppH reveals the presence of dimers that interact strongly through NH···N contacts, which results in a disorder of the NH atoms over two positions and a delocalised binding situation.[14] As a consequence, the C1–N1 and C1–N2 bond lengths (see Scheme 2 for the atom numbering) in crystalline hppH are almost equal (133.1 and 132.8 pm), whereas C1–N3 is significantly longer (136.7 pm). [(hppH)$_2$NiCl$_2$] has already been synthesised by treating (hpp)$_3$SiMe with NiCl$_2$(py)$_4$ (py = pyridine) in toluene at room temperature and has been shown to feature a more or less tetrahedrally coordinated Ni atom.[15] Furthermore, the reaction between [PdCl$_2$(cod)] (cod = cyclooctadiene) and hppH in CH_2Cl_2 affords *trans*-[(hppH)$_2$PdCl$_2$].[16] Fast isomerisation seems to occur from a *cis* arrangement of the chlorido ligands to a more stable *trans* configuration during the course of the reaction such that it proved impossible to isolate the *cis* isomer. It has been shown that the *cis* structure can only be realized if the chelating bis(guanidine) H$_2$C(hpp)$_2$ is used, which leads to the formation of *cis*-[{H$_2$C(hpp)$_2$}PdCl$_2$]. Intramolecular H···Cl contacts are present in both [(hppH)$_2$NiCl$_2$] and *trans*-[(hppH)$_2$PdCl$_2$]. It should be noted that the hpp$^-$ anion, which is easily formed by removal of a proton from hppH, has in the past been shown to coordinate in an η^2-fashion to two metal atoms (preferentially in high oxidation states). Thus, treatment of Li(hpp) with PtCl$_2$ in toluene (reflux for 3 h) leads to the dinuclear complex [Pt$_2$(hpp)$_4$Cl$_2$], which has a paddlewheel structure[17,18] with Pt–Pt, Pt–Cl and average Pt–N distances of 243.85(12), 248.3(4) and 197 pm, respectively, when the crystal structure is refined in the space group *I*4/*m*.[18]

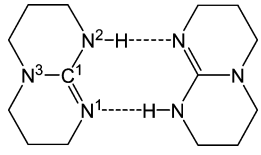

Scheme 2.

Herein we report the synthesis of [(hppH)$_2$PtCl$_2$] (**4**), which completes the series of known [(hppH)$_2$MCl$_2$] compounds (M = Ni, Pd or Pt). As opposed to the Pd complex, we were able to synthesise the complex in both its *cis* and *trans* forms by two different synthetic routes. We have also synthesised and characterised [(hppH)$_3$PtCl]$^+$Cl$^-$. Finally, the solid-state structures of some salts of the [hppH$_2$]$^+$ cation are reported, including [hppH$_2$]$_2$[PtCl$_4$].

Results and Discussion

Synthesis and Characterisation of *cis*-[(hppH)$_2$PtCl$_2$] (4a)

The synthesis of **4a** was achieved in two steps starting from K$_2$[PtCl$_4$] (see Scheme 3). The first step is the exchange of the K$^+$ cations of K$_2$[PtCl$_4$] by [hppH$_2$]$^+$, which proceeds readily in water as solvent. [hppH$_2$]$_2$[PtCl$_4$] precipitates as a pink solid from aqueous solution. The treatment of [hppH$_2$]$_2$[PtCl$_4$] with Li(hpp) in thf then affords *cis*-[(hppH)$_2$PtCl$_2$].

$$K_2[PtCl_4] + hppH + 2\,H_2O \xrightarrow{H_2O} [hppH_2]_2[PtCl_4] + 2\,K^+ + 2\,OH^-$$

$$[hppH_2]_2[PtCl_4] + 2\,Li(hpp) \xrightarrow{THF} 2\,LiCl + 2\,hppH + \textit{cis}\text{-}[(hppH)_2PtCl_2]$$

Scheme 3.

The IR spectrum of **4a** in the region around 300 cm^{-1}, which is where the Pt–Cl stretches in Pt^{II} compounds are normally found, is shown in Figure 1. The spectra of the starting reagent K$_2$[PtCl$_4$] and the [hppH$_2$]$_2$[PtCl$_4$] salt formed in the first step of the reaction are also included. The ν(Pt–Cl) stretching modes of all compounds appear near 320 cm^{-1}. The spectrum of K$_2$[PtCl$_4$] also shows absorptions in the region 200–150 cm^{-1}, which have been assigned previously to in-plane and out-of-plane deformations.[19] The ν(Pt–Cl) modes of **4a** appear at 324.2/313.9 cm^{-1}, and the in-plane and out-of-plane deformations are shifted to lower wavenumbers (approx. 130 cm^{-1}) with

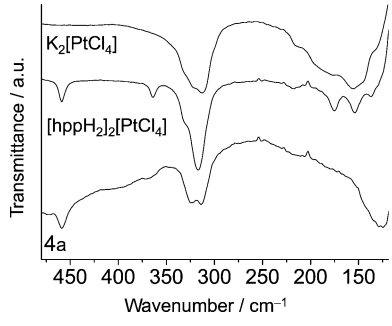

Figure 1. IR spectra of K$_2$[PtCl$_4$], [hppH$_2$]$_2$[PtCl$_4$] and **4a** in the region around 300 cm^{-1}.

respect to those of $K_2[PtCl_4]$. The absorption at 458.6 cm^{-1} is due to the hppH moiety.

The X-ray crystal structure of **4a** is illustrated in Figure 2 (top). The complex adopts a *cis* configuration with a planar $PtCl_2N_2$ core. Disorder is observed in one of the β-methylene units, which is a common feature in this type of bicyclic frameworks.[14] The relative occupancies in this case are 0.80 and 0.20, with the predominant structure consisting of an "up-down" arrangement of the β-methylene units. The Pt–Cl distances are 230.5 and 232.5 pm and the Cl–Pt–Cl and N–Pt–N angles 90.0 and 88.0°, respectively. This compares with a Pt–Cl distance of 232.8(9)/233.3(9) pm and Cl–Pt–Cl and N–Pt–N angles of 89.9 and 87(1.5)° for *cis*-$[(NH_3)_2PtCl_2]$.[1] The Pt–N distances in **4a** are 202.2 and 202.3 pm and are thus also close to those found in *cis*-$[(NH_3)_2PtCl_2]$ [205(4) and 195(3) pm, respectively].[1] Table 1 summarises some salient parameters for *cis*-$[(hppH)_2PtCl_2]$. The closest Pt···Pt separation is 694.0 pm, a value that is far too large for any significant interaction. For comparison, Pt···Pt distances of 337.2–340.9 pm are found in crystalline *cis*-$[(NH_3)_2PtCl_2]$.[1] Interestingly, the molecule features only one N–H···Cl hydrogen bond (277.2 pm). The distance between the H atom attached to N2 and Cl1 is as long as 405.1 pm. The Pt···H–N distances (270.1 and 260.8 pm) are in the region in which agostic or hydrogen bonding to Pt has been proposed for similar Pt^{II} compounds.[20] Thus, the Pt atom of the $PtCl_4$ moiety in the dianion $[\{PtCl_4\}\cdot cis\text{-}\{PtCl_2(NH_2Me)_2\}]^{2-}$ interacts with one of the hydrogen atoms attached to the N atom of the $PtCl_2(NH_2Me)_2$ part.[21,22] The Pt···HN distance was determined to be 226.2(1.1) pm by neutron diffraction techniques.[22] Another example is the complex *cis*-[Pt-{*o*-$Ph_2PC_6H_4NC(O)C_6H_4$}{*o*-$Ph_2PC_6H_4NHC(O)Ph$}] (**5**; Scheme 4),[23] where the NH···Pt distance was estimated to be 231.8(2.2) pm by X-ray diffraction. It has been debated whether these interactions can be called agostic or are simply examples of hydrogen bonding. In this context, it has been pointed out that one important criterion to answer this question is the Pt···H–N angle.[20] An angle close to 180° would suggest hydrogen bonding while a much smaller angle is necessary for an agostic interaction in which the σ-orbital of the N–H bond interacts with a suitable vacant d-orbital on the metal atom. It is difficult to judge the importance of these types of bonding in compound **4a** on the basis of these data and, unfortunately, IR data provide no answer to this question. Thus, while the ν(C–H) and ν(C=N) stretching modes appear as relatively sharp absorptions with maxima at 2955/2870 and 1630 cm^{-1}, the ν(N–H) stretches give rise to a broad absorption centred around 3320 cm^{-1}. We were thus not able to distinguish between the two N–H groups in the molecule. It is likely that the presence of the N5H···Cl contact forces this H atom to come close to the Pt atom, so it is likely that the N5H···Pt interaction plays a very minor role in **4a**. We are also not in a position to judge the importance of the N2H···Cl contact. Figure 3 (top) illustrates the packing of **4a** in the crystals. Besides the intramolecular NH···Cl contacts found for each of the molecules, the second Cl atom is engaged in one in-

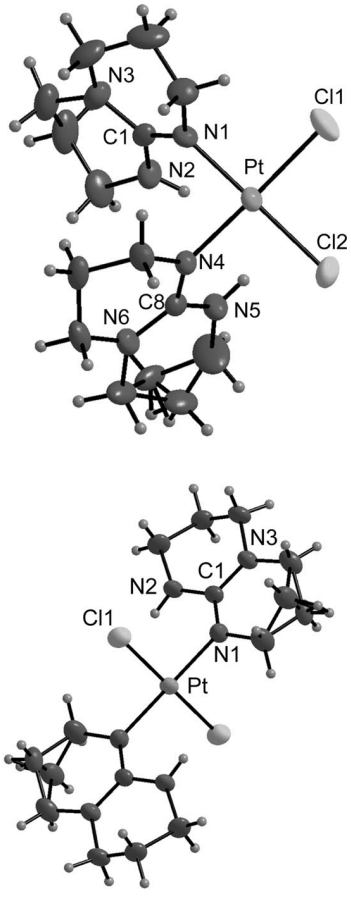

Figure 2. Structures of **4a** (top) and **4b** (bottom) determined by X-ray diffraction in the solid state.

Table 1. Salient bond lengths [pm] and angles [°] for *cis*-$[(hppH)_2PtCl_2]$ (**4a**) in the crystalline state.

Pt–Cl1	230.50(12)	C8–N5	135.7(5)
Pt–Cl2	232.36(12)	C8–N6	133.4(5)
Pt–N1	202.3(3)	Cl2···HN5	277.2(8)
Pt–N4	202.2(3)	Cl2···HN2	436.3(8)
C1–N1	131.8(5)	Cl1···HN2	405.1(7)
C1–N2	134.8(5)	Cl1···HN5	428.0(7)
C1–N3	133.4(5)	Pt···HN2	270.1(1)
C8–N4	132.8(5)	Pt···HN5	260.8(1)
Cl1–Pt–Cl2	90.0(5)	N1–C1–N2	118.6(4)
N1–Pt–N4	87.97(13)	N4–C8–N5	117.3(4)
Cl1–Pt–N1	90.37(10)	N5–H···Cl2	118.7(3)
Cl2–Pt–N4	91.63(9)	N2–H···Cl2	137.3(10)
N2–H···Pt	112.9(9)	N5–H···Cl1	145.7(3)
N5–H···Pt	118.3(1)	N2–H···Cl1	115.6(9)

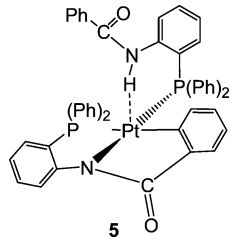

5

Scheme 4.

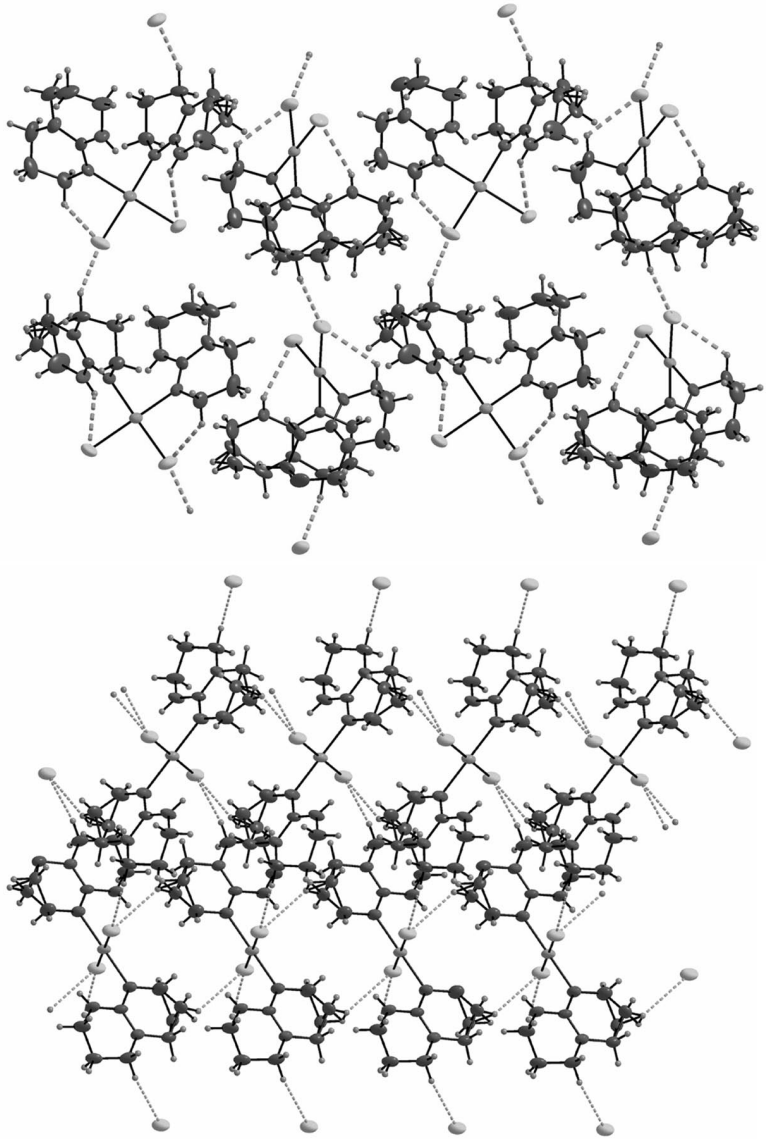

Figure 3. Illustration of the packing of molecules of **4a** (top) and **4b** (bottom) in the solid state.

tramolecular and one intermolecular CH···Cl contact. The intermolecular CH···Cl contacts are 259.4 pm and the intramolecular ones 274.5 pm.

Synthesis and Characterisation of *trans*-[(hppH)$_2$PtCl$_2$] (4b)

The *trans* isomer is more stable than the *cis* form (see below), and its synthesis is also more straightforward: It can be obtained directly from the reaction between [(dmso)$_2$-PtCl$_2$] (prepared from dmso and K_2PtCl_4 according to the literature[24]) and hppH (see Scheme 5). The NMR spectra of **4b** show only slight differences with those of **4a**, so it is virtually impossible to distinguish **4a** and **4b** by NMR spectroscopy. Interestingly, however, the ESI$^+$ mass spectra provide some differences. Thus, while the base peak in the spectrum of **4a** appears at *m*/*z* = 684.3 [(hppH)$_2$(hppH$_2$)-PtCl$_2$]$^+$, the base peak in the spectrum of **4b** appears at *m*/*z* = 647.3 [(hppH)$_3$PtCl]$^+$. Both molecules therefore seem to interact with one additional hppH molecule in solution, and the *trans* complex easily loses one chlorine atom, whereas the *cis* complex does not. The structure of an individual molecule of **4b**, as determined by X-ray diffraction, is shown in Figure 2 (bottom). Table 2 includes some salient structural parameters for this complex. As opposed to **4a**, no intramolecular NH···Cl interaction is present in **4b** (the shortest NH···Cl separations are 283 and 400 pm), whereas the Pt···HN distances of 259 pm are well within the range for hydrogen or agostic bonding. The Pt···H–N angle is around 121°, which would argue for an agostic interaction; however, we are not in a position to judge the importance and strength of these interactions. Figure 3 (bottom) illustrates the packing of molecules of **4b** in the solid state. Each Cl atom establishes two CH···Cl contacts such that adjacent molecules in each row [see Figure 3 (bottom)] are connected through two such contacts and the other two contacts link molecules in neighbouring rows.

$$[(dmso)_2PtCl_2] + 2\ hppH \longrightarrow \textit{trans}\text{-}[(hppH)_2PtCl_2] + 2\ dmso$$

Scheme 5.

Table 2. Salient bond lengths [pm] and angles [°] for *trans*-$[(hppH)_2PtCl_2]$ (**4b**) in the crystalline state.

Pt–Cl1	229.99(8)	Cl1···HN2′	400.3(23)
Pt–N1	203.3(2)	Cl1···HN2	283.1(23)
C1–N1	130.8(3)	Pt···HN2	259.4(23)
C1–N2	136.9(4)		
C1–N3	135.2(3)		
Cl1–Pt–Cl1′	180.0	N1–C1–N2	119.5(2)
N1–Pt–N1′	180.0	Pt···H–N2	121.4(93)
Cl1–Pt–N1	90.77(7)	Cl1···H–N2	129.9(93)
Cl1–Pt–N1′	89.23(7)	Cl1′···H–N2	102.8(93)

Synthesis and Characterisation of $[(hppH)_3PtCl]^+Cl^-$ (6)

We have shown that synthetic routes can be found leading either to *trans*- or to *cis*-$[(hppH)_2PtCl_2]$. However, it proved impossible to find a preparation route which did not give, in addition to one of these products, the salts $[(hppH)_3PtCl]^+Cl^-$ (especially in the preparation of **4b**) and $[hppH_2]^+Cl^-$. In reactions with smaller amounts of hppH coordination of only one hppH molecule predominated, and it also proved extremely difficult to separate the three species by means other than by crystal picking. Crystals of $[(hppH)_3PtCl]^+Cl^-$ were grown from acetone/hexane mixtures. Figure 4 displays the structure of one molecule of **6** in the solid state, as determined by X-ray diffraction. As anticipated, the Pt atom and the four directly bound atoms (three N and one Cl atom) are located in one plane. The Cl^- anion (Cl2) is coordinated to the three H atoms attached to the N atoms of the three hppH ligands [with Cl2···H distances of 243.5(9), 257.1(9) and 258.9(9) pm]. Additionally, Cl2 interacts weakly with two H atoms of methylene groups from hppH ligands of adjacent molecules of **6**. The Pt–Cl1 distance is 230.9(23) pm and is thus almost identical to those found in **4a** and **4b**. The three Pt···HN distances are 266.2(1), 277.5(1) and 277.8(1) pm and the Pt···H–N angles are 118.6(1.1), 115,7(1) and 113.9(1)°, respectively.

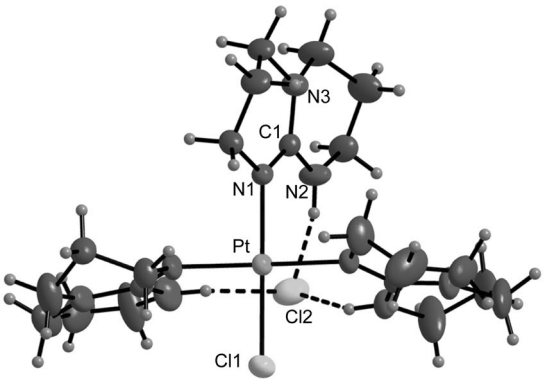

Figure 4. Structure of **6** determined by X-ray diffraction.

Synthesis and Characterisation of $[hppH_2]_2[PtCl_4]$

Figure 1 contains an IR spectrum of this salt. This spectrum consists of a strong band with a maximum at 316.7 cm^{-1} and a shoulder at about 329 cm^{-1}, which can be assigned to the ν(Pt–Cl) modes. A weak band at 354 cm^{-1} belongs to a vibration of the $[hppH_2]^+$ cation. In-plane and out-of plane deformations of the $[PtCl_4]^{2-}$ dianion are clearly visible at 175.1, 153.9 and 136.7 cm^{-1}. This compound was also identified and characterised by elemental analysis, mass spectrometry and NMR spectroscopy. Crystals suitable for X-ray diffraction analysis were grown from hot H_2O. Figure 5 clearly shows that the Cl atoms of the $[PtCl_4]^{2-}$ units in the crystalline phase of $[hppH_2]_2[PtCl_4]$ interact with the H atoms attached to the N atoms in the $[hppH_2]^+$ cations. The four Pt–Cl distances fall in the range 230.8–231.4 pm and the four Cl···H interactions in the range 239.6–256.8 pm.

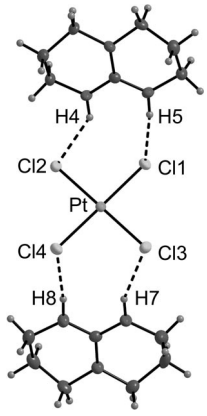

Figure 5. Structure of $[hppH_2]_2[PtCl_4]$ determined by X-ray diffraction.

Structures of Other Salts of the Guanidinium Cation {$[hppH_2]A$, where A^- is BPh_4^-, Cl^- or $Cl^-(H_2O)$}

Several structures of compounds featuring the $[hppH_2]^+$ cation, for example $[hppH_2]^+[O_2NCHPh]^-$,[25] $[hppH_2]^+[O_2CCH_3]^-$, $[hppH_2]^+[O_2CCF_3]^-$[26] and $[\{hppH_2\}^+]_3[\{TaCl_6\}^-]_2[Cl]^-$, are already known.[27] Some of these are of interest for the study of reactions involving hppH as a catalyst, such as the Michael addition of nitroalkanes,[25] or as models for hydrogen bonding in nature. Herein we present the structures of the salts $[hppH_2]^+[BPh_4]^-$, $[hppH_2]^+Cl^-$ and $[hppH_2]^+Cl^-\cdot H_2O$, which have not yet been reported. The structure of $[hppH_2]^+[BPh_4]^-$, which is depicted in Figure 6, is a good example of a compound featuring isolated $[hppH_2]^+$ cations that interact only very weakly with the borate counterions. The C1–N1 and C1–N2 bond lengths are 133.5 and 134.9 pm, respectively, and the C1–N3 bond is significantly shorter 132.6 pm. These parameters are compared to those calculated for the $[hppH_2]^+$ cation in the absence of any anion and also for the neutral hppH mole-

Table 3. Salient bond lengths [pm] and angles [°] observed and calculated (B3LYP/TZVPP) for hppH and several salts containing the $[hppH_2]^+$ cation.

	hppH[a]		$[hppH_2]^+$			
	obsd.	calcd.	$[BPh_4]^-$	Cl^-	$Cl^-\cdot H_2O$	calcd.
C1–N1	132.8[2]	128.5	133.5(7)	133.5(3)	133.78(18)	134.2
C1–N2	133.1[2]	138.9	134.9(7)	133.4(3)	133.1(2)	134.3
C1–N3	136.7[3]	138.2	132.6(7)	133.4(2)	133.44(17)	133.3
N1–C1–N2	117.90[14]	117.6	117.4(5)	118.12(18)	118.72(13)	118.7

[a] Note that hppH forms dimeric units in the solid state. The calculations were carried out for the monomer.

cule in Table 3. The difference between calculated and crystal data for hppH is due to the intermolecular interactions (dimerization) in the crytalline phase.

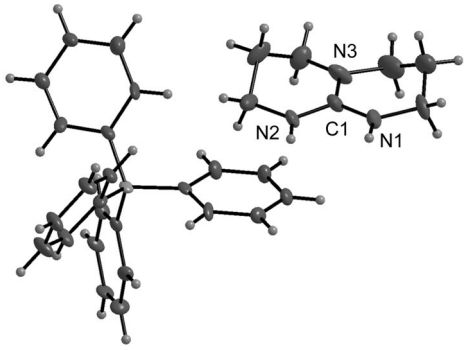

Figure 6. Structure of $[hppH_2][BPh_4]$ determined by X-ray diffraction.

Figure 7 shows the structure of $[hppH_2]^+Cl^-$, in which N–H···Cl and weaker C–H···Cl contacts involving the Cl^- anions result in a ladder-type structure. Each of the Cl atoms is surrounded by four H atoms in a distorted tetrahedral fashion. Two of these H atoms are attached to the N atoms and the other two are from α- and γ-methylene groups of the $[hppH_2]^+$ moieties. The Cl···HN and Cl···HC contacts can be estimated to be 245.7/235.4 and 279.1/277.5 pm from the X-ray diffraction data. The bond lengths between the three N atoms and the central C atom in the $[hppH_2]^+$ cations are summarised in Table 3.

$[hppH_2]^+Cl^-$ is highly hygroscopic; therefore, it was not difficult to obtain crystals in which equimolar quantities of H_2O are present. The resulting structure (see Figure 8) contains helical $Cl^-\cdot H_2O$ chains connected to each other by

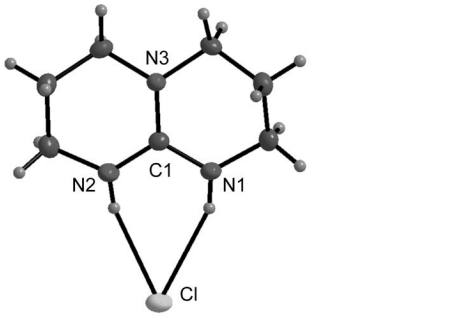

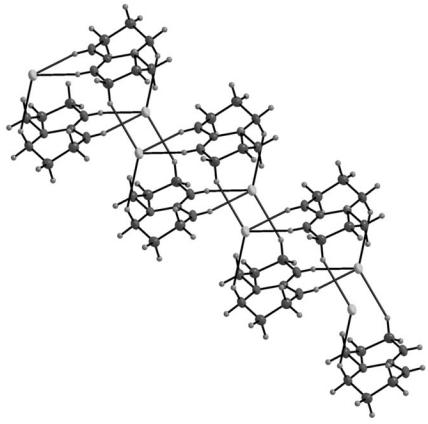

Figure 7. Structure of an individual molecule and an ensemble of molecules of $[hppH_2]Cl$ in the crystalline state, as measured by X-ray diffraction.

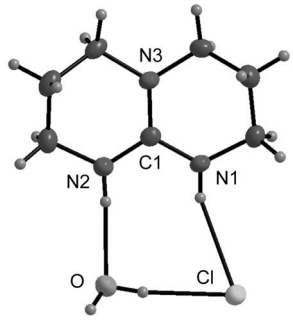

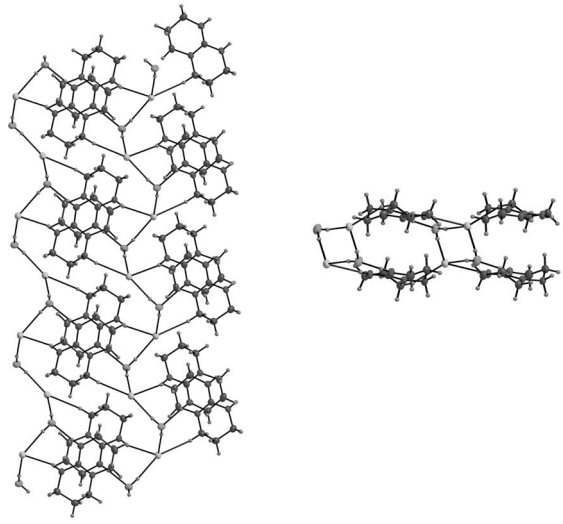

Figure 8. Structure of an individual molecule and an ensemble of molecules of $[hppH_2]Cl\cdot H_2O$ in the crystalline state, as measured by X-ray diffraction.

hydrogen bonding with the $[hppH_2]^+$ cations. A view along the direction of these chains is also shown in Figure 8 where the chains now appear as rhombohedral channels and the layer structure of the $[hppH_2]^+$ cations is visible. Each of the Cl^- anions is fivefold coordinated by two hydrogen atoms of water, one H atom attached to an N atom and two H atoms of methylene groups of the $[hppH_2]^+$ moieties. The Cl···HN1, O···HN2 and OH···Cl distances are 245.6, 200.0 and 221.3 pm, respectively.

Quantum Chemical Calculations

Quantum chemical calculations were carried out for the *cis* and *trans* isomers of $[(hppH)_2PdCl_2]$ and $[(hppH)_2PtCl_2]$ and also for $[(NH_3)_2PtCl_2]$ to validate the quality of our calculations. The *trans* isomer was lower in energy in all cases. Using BP86 and the def2-TZVPP basis set for all atoms, we calculated a *trans*–*cis* energy difference of –47 kJ mol^{-1} for $[(NH_3)_2PtCl_2]$, whereas when B3LYP is applied together with the same basis sets the energy difference increases slightly to –52 kJ mol^{-1}. These values compare with values of –55 kJ mol^{-1} calculated previously with B3LYP[2] or MP2,[4] –76 kJ mol^{-1} calculated with HF[3] and –57 kJ mol^{-1} obtained with the G3 scheme.[4] According to our B3LYP calculations, a single molecule of cisplatin has Pt–Cl and Pt–N bond lengths of 230.6 and 210.9 pm, respectively. The Pt–Cl and Pt–N distances are 232.8/233.3 and 205/195 pm, respectively, in the solid state.[1] Interestingly, one of the N–H bonds of each NH_3 group in the calculated structure is slightly longer than the others (102.3 vs. 101.5 pm) and the H atom of these elongated N–H bonds is only 252.4 pm away from the Pt atoms. However, the reason for this small distance is likely to be the presence of an NH···Cl contact of 241.0 pm rather than a significant NH···Pt interaction. The other NH···Pt distances are 269.3 pm. The Pt–Cl and Pt–N distances in *trans*-$[(NH_3)_2PtCl_2]$ were calculated to be 233.4 and 206.0 pm, respectively, compared to values of 232 and 205 pm determined from single-crystal X-ray diffraction experiments.[1]

One *trans* form and two *cis* forms were calculated for both $[(hppH)_2PdCl_2]$ and $[(hppH)_2PtCl_2]$. The *cis* forms differ in the arrangement of the hppH ligands and feature different symmetries (C_2 and C_1, denoted *cis*-II and *cis*-I). As anticipated, and in line with the experimental results for $[(hppH)_2PdCl_2]$,[16] the calculations predict the *trans* form to be more stable than the *cis* form for both the Pt and the Pd complexes. Among both *cis* forms, the more symmetrical isomer (C_2) is lower in energy. The energy gap between the *trans* and the more stable *cis* form for $[(hppH)_2PdCl_2]$ is calculated to be 31 and 32 kJ mol^{-1} with BP86 and B3LYP, respectively. The respective values for the energy difference between the two *cis* isomers are 8 and 9 kJ mol^{-1}, hence the *cis*–*trans* energy difference is much lower than in $[(NH_3)_2PtCl_2]$. In contrast to NH_3, the hppH ligand is a (weak) π-donor. Figure 9 shows the *trans* and lower-lying *cis* structures, while Table 4 lists some salient parameters for all three isomers. The dimensions calculated for the *trans* form are in good agreement with the experimentally obtained values, although in certain cases the calculated distances are longer than the measured ones. For example, the calculated Pd–Cl and Pd–N distances (236.2 and 205.9 pm, respectively) are longer than the experimentally determined ones of 233.1/232.2 and 203.7/201.1 pm.[16]

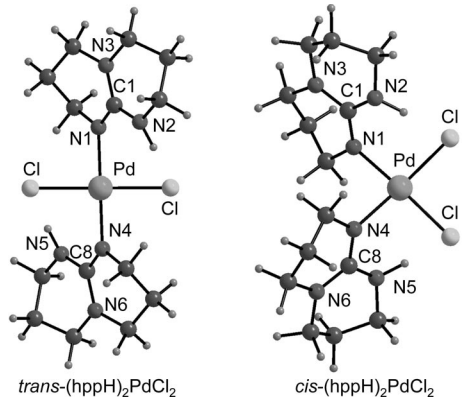

Figure 9. Calculated structures for *trans*- and *cis*-*II*-$[(hppH)_2PdCl_2]$.

Table 4. Salient bond lengths [pm] and angles [°] calculated (B3LYP) for the *trans* and *cis* forms of $[(hppH)_2PdCl_2]$ and $[(hppH)_2PtCl_2]$. See Figures 9 and 10 for the atom numbering.

	$[(hpph)_2PdCl_2]$			$[(hpph)_2PtCl_2]$		
	trans	*cis*-I	*cis*-II	*trans*	*cis*-I	*cis*-II
M–Cl1	236.2	231.6	232.8	236.0	232.4	233.6
M–Cl2	236.2	233.4	232.8	236.0	233.9	233.6
M–N1	205.9	208.1	208.7	206.3	207.9	207.9
M–N4	205.9	209.5	208.7	206.3	208.8	207.9
C1–N1	131.0	131.1	131.0	131.2	131.1	131.2
C1–N2	136.1	136.0	136.6	135.9	135.8	136.5
C1–N3	136.8	136.6	137.0	136.9	137.3	136.9
C8–N4	131.0	130.9	131.0	131.2	131.0	131.2
C8–N5	136.1	136.9	136.6	135.9	137.1	136.5
C8–N6	136.8	137.0	137.0	136.9	137.5	136.9
N2–H	101.6	101.0	101.8	101.3	101.2	101.5
N5–H	101.6	102.1	101.8	101.3	101.7	101.5
N2H···Cl1	227.8	329.3	231.1	234.0	373.6	245.3
N5H···Cl2	227.8	223.9	231.1	234.1	239.9	245.3
N2H···M	271.1	246.3	261.7	268.7	248.0	256.1
N5H···M	271.2	263.6	261.8	268.7	254.1	256.1
Cl1–M–Cl2	180.0	92.2	91.2	180.0	92.0	91.5
N1–M–N4	180.0	90.7	88.4	180.0	91.7	89.3
Cl1–M–N1	91.2	86.5	90.3	91.3	87.1	89.7
Cl2–M–N4	91.2	90.6	90.3	91.3	89.3	89.7
N1–C1–N2	119.3	118.6	118.5	119.4	118.8	118.7
N4–C8–N5	119.3	118.5	118.5	119.4	118.4	118.7
N2–H···M	109.3	121.9	116.2	112.0	122.2	119.2
N5–H···M	109.3	114.1	116.2	112.0	120.1	119.2

The two *cis* forms of $[(hppH)_2PtCl_2]$ are illustrated in Figure 10. According to our BP86 and B3LYP calculations, the *trans* form is more stable than the lowest-energy *cis* form by 28 and 30 kJ mol^{-1}, respectively. Thus, the hppH ligand again stabilizes the *cis* form in comparison to the NH_3 ligand. The energy difference between the *cis* forms is 4 and 6 kJ mol^{-1} according to BP68 and B3LYP, respectively. We can therefore state that *cis*-I and *cis*-II have almost identical energies. The conformation of the two hppH

ligands in *cis*-I is close to that observed in our experiments in that only one Cl···HN contact is established; two such contacts are present in *cis*-II. The hypothetical displacement reaction set out in Scheme 6 is calculated to be associated with an energy change of –68 kJ mol^{-1} according to BP86 and –62 kJ mol^{-1} according to B3LYP (*cis*-I isomer). The zero-point-corrected energy and the standard Gibbs energy changes are –82 and –58 kJ mol^{-1} according to BP86 and –76 and –53 kJ mol^{-1} according to B3LYP.

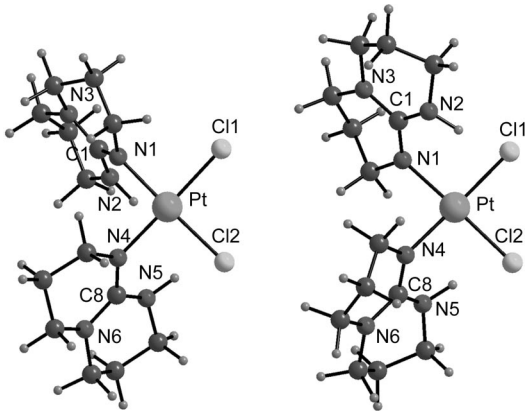

Figure 10. The two calculated minimum structures of *cis*-[(hppH)$_2$PtCl$_2$] (*cis*-I on the left and *cis*-II on the right).

cis-[(NH$_3$)$_2$PtCl$_2$] + 2 hppH ⟶ *cis*-[(hppH)$_2$PtCl$_2$] + 2 NH$_3$

Scheme 6.

We calculated a reaction energy of –53 (BP86) and –46 kJ mol^{-1} (B3LYP) for the hypothetical base-exchange reaction starting with *trans*-[(NH$_3$)$_2$PtCl$_2$] and leading to *trans*-[(hppH)$_2$PtCl$_2$]. The calculated structure of the *trans* form (see Table 4) deviates in some aspects from the experimentally determined one in the solid state. Thus, the calculated intramolecular N–H···Cl and Pt···H–N distances of 234.0 and 268.7 pm suggest significant N–H···Cl interactions. According to the X-ray diffraction analysis, the N–H···Cl separations are larger in the solid state, whereas the Pt···H–N distances are of the same order (approx. 265 pm). The intermolecular C–H···Cl interactions are presumably responsible for these deviations.

Conclusions

This work reports the first synthesis of *cis*- and *trans*-[(hppH)$_2$PtCl$_2$] (hppH = 1,3,4,6,7,8-hexahydro-2*H*-pyrimido[1,2-*a*]pyrimidine). The intermolecular CH···Cl contacts formed in the solid state for *cis*-[(hppH)$_2$PtCl$_2$] are presumably responsible for the conformation of the hppH ligands in which only one intramolecular NH···Cl contact is established. The synthesis of *cis*-[(hppH)$_2$PtCl$_2$] has been achieved in two steps involving formation of the salt [hppH$_2$]$_2$[PtCl$_4$] from K$_2$[PtCl$_4$] and hppH in the first step and its subsequent reaction with Li(hpp). Alternative synthetic routes failed to give the desired product. *trans*-[(hppH)$_2$PtCl$_2$] is obtained in a more straightforward manner by treating [(dmso)$_2$PtCl$_2$] with hppH. The crystal structure of this complex provides evidence for intermolecular C–H···Cl contacts but no intramolecular N–H···Cl interactions, although the distances suggest the presence of some Pt···H–N bonding. Quantum chemical calculations have shed additional light on the possible structures and properties of [(hppH)$_2$PtCl$_2$] in its *cis* and *trans* configurations. [(hppH)$_3$PtCl]$^+$Cl$^-$ and [hppH$_2$]Cl are formed as side products in the preparation of *cis*- and *trans*-[(hppH)$_2$PtCl$_2$]. We have also reported the solid-state structures of the salt [hppH$_2$]$_2$[PtCl$_4$] and the Pt-free salts [hppH$_2$][BPh$_4$], [hppH$_2$]Cl and [hppH$_2$]Cl·H$_2$O. While directed intermolecular contacts are of minor importance in [hppH$_2$][BPh$_4$], hydrogen bonding leads to ladder-type networks and helical chain architectures in the other two salts.

Experimental Details

General: All synthetic work was carried out using standard Schlenk techniques. IR spectra were recorded with a Bruker Vertex 80v spectrometer, and NMR spectra were recorded with a Bruker Avance II 400 spectrometer. A Perkin–Elmer Lambda 19 spectrometer was used for UV/Vis spectroscopy.

[hppH$_2$]$_2$[PtCl$_4$]: hppH (Fluka, ≥98% purity; 104 mg, 0.75 mmol) was added to a solution of K$_2$[PtCl$_4$] (ABCR, 99.9% purity; 104 mg, 0.25 mmol) in about 1 mL of H$_2$O. The bright red precipitate that formed immediately was separated from the solution by filtration and washed with small portions of H$_2$O (0.5–1 mL), EtOH (0.5–1 mL), toluene and diethyl ether. It was then dried in vacuo to give 123 mg (0.2 mmol) of a bright red powder (80% yield). Recrystallisation of the product from H$_2$O yielded orange crystals. C$_{14}$H$_{28}$Cl$_4$N$_6$Pt (617.31): calcd. C 27.24, H 4.57, Cl 22.97, N 13.61; found C 27.28, H 4.48, Cl 22.87, N 13.32. MS (ESI$^-$, CH$_3$CN): *m*/*z* (%) = 476 (80) [(hppH)(PtCl$_4$)]$^-$, 440 (18) [(hppH)(PtCl$_3$)]$^-$. ^{1}H NMR (400 MHz, [D$_6$]dmso): δ = 1.87 (q, $^3J_{HH}$ = 5.8 Hz, 8 H, CH$_2$), 3.18 (m, 8 H, CH$_2$), 3.27 (t, $^3J_{HH}$ = 5.9 Hz, 8 H, CH$_2$), 7.77 (s, 4 H, NH) ppm. ^{13}C NMR (101 MHz, [D$_6$]dmso): δ = 150.64, 46.10, 37.37, 20.17 ppm. ^{195}Pt NMR (86 MHz, [D$_6$]dmso): δ = –2954.03 ppm. UV/Vis (solid): λ = 238, 335, 397, 485 nm.

***cis*-[(hppH)$_2$PtCl$_2$] (4a):** 10 mL of dry thf was added to [hppH$_2$]$_2$[PtCl$_4$] (84 mg, 0.136 mmol). Li(hpp) (0.544 mmol, 4 equiv.), prepared as described in the literature,[18] was then slowly added to this suspension with a syringe. The solution turned clear yellow and was stirred for an additional 15 min, then the solvent was removed in vacuo. The pale-yellow oily residue was washed two or three times with toluene and filtered through a 1-cm silica frit. The residue was washed from the frit with CH$_2$Cl$_2$ and the solvent removed in vacuo to yield 137 mg of a pale-yellow powder, which consists of the product and the [hppH$_2$]Cl salt. Layering of a CH$_2$Cl$_2$ solution with petroleum ether (boiling range 40–60 °C) gave yellow crystals of [(hppH)$_2$PtCl$_2$] together with colourless crystals of [hppH$_2$]Cl and small quantities of [(hppH)$_3$PtCl]$^+$Cl$^-$. The crystals were separated manually with a spatula for further analysis. MS (EI$^+$): *m*/*z* (%) = 544.7 (80) [M$^+$], 471.7 (22) [M$^+$ – 2 Cl – 2 H]$^+$; (ESI$^+$, CH$_3$CN): *m*/*z* (%) = 684.3 (100) [(hppH)$_2$(hppH$_2$)PtCl$_2$]$^+$, 648.4 (80) [(hppH)$_3$PtCl(H)]$^+$. ^{1}H NMR (400 MHz, CD$_2$Cl$_2$): δ = 1.83 (q, $^3J_{HH}$ = 5.8 Hz, 4 H, 6-H), 1.89 (q, $^3J_{HH}$ = 5.9 Hz, 4 H, 3-H), 3.14 (t, $^3J_{HH}$ = 6.1 Hz, 4 H, 5-H), 3.19 (t, $^3J_{HH}$ = 6.1 Hz, 4 H, 4-H), 3.28 (m, 4 H, 2-H) 3.38 (t, $^3J_{HH}$

= 5.7 Hz, 4 H, 7-H), 6.67 (s, 2 H, 1-H) ppm. ^{13}C NMR (101 MHz, CD_2Cl_2): δ = 22.72 (C3), 23.42 (C6), 39.79 (C2), 47.43 (C5), 48.40/48.56 (C4/C7) ppm.

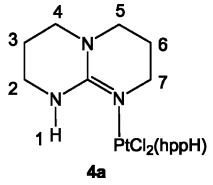

4a

***trans*-[(hppH)$_2$PtCl$_2$] (4b):** [(dmso)$_2$PtCl$_2$][24] (71 mg, 0.168 mmol) and hppH (72 mg, 0.518 mmol) were dissolved in 15 mL of CH_2Cl_2. The resulting pale-yellow solution was stirred at room temperature for 20 h. The solvent was then removed in vacuo, and the pale-yellow oily residue was washed two or three times with toluene and filtered through a 1-cm silica frit. The residue was washed from the frit with CH_2Cl_2, and the solvent was again removed to give 76 mg of a pale-yellow powder. Crystals were obtained by layering an acetone solution of this powder with hexane. MS (ESI$^+$, CH_3CN): *m*/*z* = 647.3 [(hppH)$_3$PtCl]$^+$; (EI$^+$): *m*/*z* = 544 [M]$^+$. ^{1}H NMR (400 MHz, CD_2Cl_2): δ = 1.84 (q, $^3J_{HH}$ = 6.9 Hz, 4 H, 6-H), 1.91 (q, $^3J_{HH}$ = 5.9 Hz, 4 H, 3-H), 3.11 (t, $^3J_{HH}$ = 6.1 Hz, 4 H, 5-H), 3.17 (t, $^3J_{HH}$ = 6.1 Hz, 4 H, 4-H), 3.30 (m, 4 H, 2-H), 3.40 (t, $^3J_{HH}$ = 5.7 Hz, 4 H, 7-H), 6.37 (s, 2 H, 1-H) ppm. ^{13}C NMR (101 MHz, CD_2Cl_2): δ = 22.07 (C3), 22.69 (C6), 39.81 (C2), 47.30/47.39 (C5/C7), 48.27 (C4) ppm.

[(hppH)$_3$PtCl]$^+$Cl$^-$ (6): This salt was obtained as a by-product of the synthesis of **4b** (and also, to a lesser extent, of **4a**). MS (ESI$^+$, CH_3CN): *m*/*z* = 647.4 [M]$^+$. ^{1}H NMR (400 MHz, CD_2Cl_2): δ = 1.80–1.89 (m, 3-H and 6-H), 3.14–3.22 (m, 4-H and 5-H), 3.33 (m, 2-H and 7-H), 6.82 (s, 1-H) ppm. ^{13}C NMR (101 MHz, CD_2Cl_2): δ = 22.73/23.29 (C3 and C6), 39.55/39.73 (C2), 47.43/47.54 (C4), 48.53/48.57/48.76 (C5 and C7), 152.29 (C1) ppm.

[hppH$_2$]Cl: This compound was obtained as a co-product of the synthesis of both *cis*- and *trans*-[(hppH)$_2$PtCl$_2$] and was separated manually from the crystalline mixture with a spatula for further analysis. ESI$^+$ (CH_3CN): *m*/*z* = 315.2 [(hppH$_2$)$_2$Cl]$^+$. ^{1}H NMR (200 MHz, $CDCl_3$): δ = 2.01 (q, $^3J_{HH}$ = 5.9 Hz, 4 H, CH_2), 3.29 (m, 8 H, CH_2), 8.75 (s, 2 H, NH) ppm. ^{13}C NMR (50 MHz, $CDCl_3$): δ = 20.69, 37.87, 46.83 ppm. ^{13}C NMR (101 MHz, CD_2Cl_2): δ = 21.21, 38.41, 47.21, 152.20 ppm.

[hppH$_2$][BPh$_4$]: Crystals of this compound were grown from toluene. Intensity data for a weakly diffracting pseudo-merohedrally twinned crystal were collected at 100 K with a Bruker AXS Smart 1000 CCD diffractometer (Mo-K_α radiation, graphite monochromator, λ = 0.71073 Å). Data were corrected for Lorentz, polarisation and absorption effects (semiempirical, SADABS). De-twinning of the reflections was effected with DIRAX. The structure was solved by direct methods and refined by full-matrix least-squares methods based on F^2 with all measured unique reflections. All non-hydrogen atoms were given anisotropic displacement parameters. All hydrogen atoms on carbon atoms were set at calculated positions and refined with a riding model. The positions of the two hydrogen atoms on N were determined from the difference Fourier synthesis. The N–H bond lengths were restrained during refinement to be equal within 0.02 Å.

X-ray Crystallographic Study: Suitable crystals were taken directly out of the mother liquor, immersed in perfluorinated polyether oil, and fixed on top of a glass capillary. Measurements were made with a Nonius-Kappa CCD diffractometer equipped with a low-temperature unit using graphite-monochromated Mo-K_α radiation. The temperature was set to 200 K. The data collected were processed using the standard Nonius software.[28] All calculations were performed using the SHELXT-PLUS software package. Structures were solved by direct methods with the SHELXS-97 program and refined with the SHELXL-97 program.[29,30] Graphical handling of the structural data during solution and refinement was performed with XPMA.[31] Structural representations were generated using Winray 32.[32] Atomic coordinates and anisotropic thermal parameters of non-hydrogen atoms were refined by full-matrix least-squares calculations. CCDC-659355 {[hppH$_2$][BPh$_4$]}, -659356 {[hppH$_2$]Cl·H$_2$O}, -659357 {[hppH$_2$]Cl}, -659358 {*cis*-[(hppH)$_2$-PtCl$_2$] (**4a**)}, -659359 {[(hppH)$_3$PtCl]$^+$Cl$^-$ (**6**)}, -659360 {[hppH$_2$]$_2$-[PtCl$_4$]} and -659361 {*trans*-[(hppH)$_2$PtCl$_2$] (**4b**)} contain the supplementary crystallographic data for this paper. These data can be obtained free of charge from The Cambridge Crystallographic Data Centre via www.ccdc.cam.ac.uk/data_request/cif.

Details of the Quantum Chemical Calculations: All calculations were performed with the aid of the TURBOMOLE program package[33] within the framework of density functional theory. The BP86 functional[34] (BP is the short notation for Becke–Perdew and is a gradient-corrected DFT method employing the Becke exchange and Perdew correlation functionals) as well as the B3LYP hybrid functional[35] were applied. The def2-TZVPP basis set was chosen for all atoms.[36] This requires the use of effective core potentials[37] for Pd and Pt. To obtain thermochemical data, further calculations with the B3LYP functional using the small def2-SVP basis set[36] were carried out, including a vibrational analysis. These thermochemical corrections were added to both the BP86 and B3LYP results. All optimised structures proved to be minima.

Acknowledgments

The authors thank the Deutsche Forschungsgemeinschaft and the Fonds der Chemischen Industrie for their continuing financial support.

[1] G. H. W. Milburn, M. R. Truter, *J. Chem. Soc. A* **1966**, 1609–1616.
[2] N. S. Panina, A. N. Beljaev, S. A. Simanova, M. Calligaris, *Int. J. Quantum Chem.* **2004**, *96*, 80–88.
[3] H. Basch, M. Krauss, J. Stevens, D. Cohen, *Inorg. Chem.* **1985**, *24*, 3313–3317.
[4] J. V. Burda, M. Zeizinger, J. Sponer, J. Leszczynski, *J. Chem. Phys.* **2000**, *113*, 2224–2232.
[5] J. Cooper, T. Ziegler, *Inorg. Chem.* **2002**, *41*, 6614–6622.
[6] T. G. Appleton, J. R. Hall, S. F. Ralph, *Inorg. Chem.* **1985**, *24*, 4685–4693.
[7] H. J. S. King, *J. Chem. Soc.* **1948**, 1912.
[8] R. A. Periana, D. J. Taube, S. Gamble, H. Taube, T. Satoh, H. Fujii, *Science* **1998**, *280*, 560–564.
[9] W. B. Connick, R. E. Marsh, W. P. Schaefer, H. B. Grey, *Inorg. Chem.* **1997**, *36*, 913–922.
[10] L. Johansson, O. B. Ryan, M. Tilset, *J. Am. Chem. Soc.* **1999**, *121*, 1974–1975.
[11] K. Mylvaganam, G. B. Bacskay, N. S. Hush, *J. Am. Chem. Soc.* **2000**, *122*, 2041–2052.
[12] R. Schwesinger, *Chimia* **1985**, *39*, 269–272.
[13] R. T. Boeré, V. Klassen, G. Wolmerhäuser, *J. Chem. Soc. Dalton Trans.* **1998**, 4147–4154.
[14] S. H. Oakley, D. B. Soria, M. P. Coles, P. B. Hitchcock, *Dalton Trans.* **2004**, 537–546.
[15] S. H. Oakley, D. B. Soria, M. P. Coles, P. B. Hitchcock, *Polyhedron* **2006**, *25*, 1247–1255.
[16] S. H. Oakley, M. P. Coles, P. B. Hitchcock, *Inorg. Chem.* **2004**, *43*, 7564–7566.

[17] R. Clérac, F. A. Cotton, L. M. Daniels, J. P. Donahue, C. A. Murillo, D. J. Timmons, *Inorg. Chem.* **2000**, *39*, 2581–2584.
[18] F. A. Cotton, C. A. Murillo, X. Wang, C. C. Wilkinson, *Inorg. Chim. Acta* **2003**, *351*, 191–200.
[19] a) H. Poulet, P. Delorme, T. P. Mathieu, *Spectrochim. Acta* **1964**, *20*, 1855–1863; b) A. Sabatini, L. Sacconi, V. Schettino, *Inorg. Chem.* **1964**, *3*, 1775–1776; c) J. Hiraishi, T. Shimanouchi, *Spectrochim. Acta* **1966**, *22*, 1483–1491; d) J. Hiraishi, T. Tamura, *J. Chem. Phys.* **1977**, *66*, 3899–3902.
[20] W. Yao, O. Eisenstein, R. H. Crabtree, *Inorg. Chim. Acta* **1997**, *254*, 105–111.
[21] L. Brammer, J. M. Charnock, P. L. Goggin, R. J. Goodfellow, T. F. Koetzle, A. G. Orpen, *J. Chem. Soc. Chem. Commun.* **1987**, 443–445.
[22] L. Brammer, J. M. Charnock, P. L. Goggin, R. J. Goodfellow, A. G. Orpen, T. F. Koetzle, *J. Chem. Soc. Dalton Trans.* **1991**, 1789–1798.
[23] D. Hedden, D. M. Roundhill, W. C. Fultz, A. L. Rheingold, *Organometallics* **1986**, *5*, 336–343.
[24] R. Romeo, L. M. Scalaro, *Inorg. Synth.* **1998**, *32*, 153–158.
[25] E. van Aken, H. Wynberg, F. van Bolhuis, *J. Chem. Soc. Chem. Commun.* **1992**, 629–630.
[26] F. A. Cotton, D. J. Timmons, *Polyhedron* **1998**, *17*, 179–184.
[27] D. B. Soria, J. Grundy, M. P. Coles, P. B. Hitchcock, *Polyhedron* **2003**, *22*, 2731–2737.
[28] *DENZO-SMN, Data Processing Software*, Nonius, **1998**; http://www.nonius.com.
[29] a) G. M. Sheldrick, *SHELXS-97*, *Program for Crystal Structure Solution*, University of Göttingen, Germany, **1997**; http://shelx.uni-ac.gwdg.de/SHELX/index.html; b) G. M. Sheldrick, *SHELXL-97*, *Program for Crystal Structure Refinement*, University of Göttingen, Germany, **1997**; http://shelx.uni-ac.gwdg.de/SHELX/index.html.
[30] *International Tables for X-ray Crystallography*, Kynoch Press, Birmingham, U. K., **1974**, vol. 4.
[31] L. Zsolnai, G. Huttner, *XPMA*, University of Heidelberg, Germany, **1994**; http://www.uni-heidelberg.de/institute/fak12/AC/huttner/software/software.html.
[32] R. Soltek, *Winray 32*, University of Heidelberg, Germany, **2000**; http://www.uni-heidelberg.de/institute/fak12/AC/huttner/software/software.html.
[33] a) R. Ahlrichs, M. Bär, M. Häser, H. Horn, C. Kölmel, *Chem. Phys. Lett.* **1989**, *162*, 165–169; b) O. Treutler, R. Ahlrichs, *J. Chem. Phys.* **1995**, *102*, 346–354; c) K. Eichkorn, F. Weigend, O. Treutler, R. Ahlrichs, *Theor. Chem. Acc.* **1997**, *97*, 119–124.
[34] a) A. D. Becke, *Phys. Rev. A* **1988**, *38*, 3098–3100; b) J. P. Perdew, *Phys. Rev. B* **1986**, *33*, 8822–8824.
[35] P. J. Stephens, F. J. Devlin, C. F. Chabalowski, M. J. Frisch, *J. Phys. Chem.* **1994**, *98*, 11623–11627.
[36] F. Weigend, R. Ahlrichs, *Phys. Chem. Chem. Phys.* **2005**, *7*, 3297–3305.
[37] D. Andrae, U. Häußermann, M. Dolg, H. Stoll, H. Preuß, *Theor. Chim. Acta* **1990**, *77*, 123–141.

Received: September 7, 2007
Published Online: January 15, 2008

